molecular pharmaceutics

Article

pubs.acs.org/molecularpharmaceutics

# Factors Governing P-Glycoprotein-Mediated Drug–Drug Interactions at the Blood–Brain Barrier Measured with Positron Emission Tomography

Thomas Wanek,[†] Kerstin Römermann,[‡,§] Severin Mairinger,[†] Johann Stanek,[†,§] Michael Sauberer,[†] Thomas Filip,[†] Alexander Traxl,[†] Claudia Kuntner,[†] Jens Pahnke,[∥,⊥] Florian Bauer,[#] Thomas Erker,[#] Wolfgang Löscher,[‡] Markus Müller,[§] and Oliver Langer*[,†,§]

[†]Health & Environment Department, AIT Austrian Institute of Technology GmbH, Seibersdorf, Austria

[‡]Department of Pharmacology, Toxicology & Pharmacy, University of Veterinary Medicine Hannover, Hannover, Germany

[§]Department of Clinical Pharmacology, Medical University of Vienna, Vienna, Austria

[∥]Department of Neuro-/Pathology, University of Oslo (UiO) and Oslo University Hospital (OUS), Oslo, Norway

[⊥]Lübeck Institute of Experimental Dermatology, University of Lübeck, Lübeck, Germany

[#]Department of Medicinal Chemistry, University of Vienna, Vienna, Austria

Supporting Information

**ABSTRACT:** The adenosine triphosphate-binding cassette transporter P-glycoprotein (ABCB1/Abcb1a) restricts at the blood–brain barrier (BBB) brain distribution of many drugs. ABCB1 may be involved in drug–drug interactions (DDIs) at the BBB, which may lead to changes in brain distribution and central nervous system side effects of drugs. Positron emission tomography (PET) with the ABCB1 substrates (*R*)-[$^{11}$C]-verapamil and [$^{11}$C]-*N*-desmethyl-loperamide and the ABCB1 inhibitor tariquidar has allowed direct comparison of ABCB1-mediated DDIs at the rodent and human BBB. In this work we evaluated different factors which could influence the magnitude of the interaction between tariquidar and (*R*)-[$^{11}$C]verapamil or [$^{11}$C]-*N*-desmethyl-loperamide at the BBB and thereby contribute to previously observed species differences between rodents and humans. We performed *in vitro* transport experiments with [$^{3}$H]verapamil and [$^{3}$H]-*N*-desmethyl-loperamide in ABCB1 and Abcb1a overexpressing cell lines. Moreover we conducted *in vivo* PET experiments and biodistribution studies with (*R*)-[$^{11}$C]verapamil and [$^{11}$C]-*N*-desmethyl-loperamide in wild-type mice without and with tariquidar pretreatment and in homozygous *Abcb1a/1b*$^{(-/-)}$ and heterozygous *Abcb1a/1b*$^{(+/-)}$ mice. We found no differences for *in vitro* transport of [$^{3}$H]verapamil and [$^{3}$H]-*N*-desmethyl-loperamide by ABCB1 and Abcb1a and its inhibition by tariquidar. [$^{3}$H]-*N*-Desmethyl-loperamide was transported with a 5 to 9 times higher transport ratio than [$^{3}$H]verapamil in ABCB1- and Abcb1a-transfected cells. *In vivo*, brain radioactivity concentrations were lower for [$^{11}$C]-*N*-desmethyl-loperamide than for (*R*)-[$^{11}$C]verapamil. Both radiotracers showed tariquidar dose dependent increases in brain distribution with tariquidar half-maximum inhibitory concentrations ($IC_{50}$) of 1052 nM (95% confidence interval CI: 930–1189) for (*R*)-[$^{11}$C]verapamil and 1329 nM (95% CI: 980–1801) for [$^{11}$C]-*N*-desmethyl-loperamide. In homozygous *Abcb1a/1b*$^{(-/-)}$ mice brain radioactivity distribution was increased by 3.9- and 2.8-fold and in heterozygous *Abcb1a/1b*$^{(+/-)}$ mice by 1.5- and 1.1-fold, for (*R*)-[$^{11}$C]verapamil and [$^{11}$C]-*N*-desmethyl-loperamide, respectively, as compared with wild-type mice. For both radiotracers radiolabeled metabolites were detected in plasma and brain. When brain and plasma radioactivity concentrations were corrected for radiolabeled metabolites, brain distribution of (*R*)-[$^{11}$C]verapamil and [$^{11}$C]-*N*-desmethyl-loperamide was increased in tariquidar (15 mg/kg) treated animals by 14.1- and 18.3-fold, respectively, as compared with vehicle group. Isoflurane anesthesia altered [$^{11}$C]-*N*-desmethyl-loperamide but not (*R*)-[$^{11}$C]verapamil metabolism, and this had a direct effect on the magnitude of the increase in brain distribution following ABCB1 inhibition. Our data furthermore suggest that in the absence of ABCB1 function brain distribution of [$^{11}$C]-*N*-desmethyl-loperamide but not (*R*)-[$^{11}$C]verapamil may depend on cerebral blood flow. In conclusion, we have identified a number of important factors, i.e., substrate affinity to ABCB1, brain uptake of radiolabeled metabolites, anesthesia, and cerebral blood flow, which can directly influence the magnitude of ABCB1-mediated DDIs at the BBB and should therefore be taken into consideration when interpreting PET results.

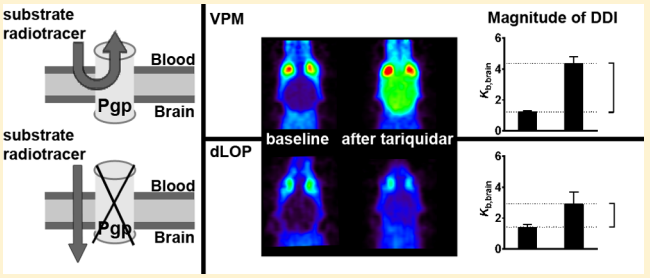


**KEYWORDS:** *P-glycoprotein, blood–brain barrier, drug–drug interaction, positron emission tomography, (R)-[$^{11}$C]verapamil, [$^{11}$C]-N-desmethyl-loperamide, tariquidar*

## INTRODUCTION

Many drugs are hindered from reaching the brain by adenosine triphosphate-binding cassette (ABC) transporters, such as

**Received:** February 25, 2015
**Revised:** June 1, 2015
**Accepted:** July 22, 2015
**Published:** July 22, 2015

  

DOI: 10.1021/acs.molpharmaceut.5b00168
*Mol. Pharmaceutics* 2015, 12, 3214–3225

P-glycoprotein (humans, ABCB1; rodents, Abcb1a) and breast cancer resistance protein (humans, ABCG2; rodents, Abcg2).[1] These transporters are expressed in the luminal membrane of brain capillary endothelial cells forming the blood−brain barrier (BBB), where they efflux their substrates into the capillary lumen. It was shown that genetic knockout of Abcb1a in mice can lead to pronounced increases in brain distribution of ABCB1 substrate drugs, such as ivermectin, digoxin, or loperamide.[2−4] Similar effects have been observed in rodent studies in which Abcb1a was inhibited with ABCB1 inhibitors, such as cyclosporine A, elacridar, zosuquidar, or tariquidar.[5−7]

ABCB1-mediated efflux transport of drugs at the BBB is of great concern in drug development as concomitant administration of multiple drugs that are recognized by ABCB1 may lead to changes in brain distribution of the drugs, compared with administration of the drugs alone (ABCB1-mediated drug−drug interaction, DDI).[1,8] This may potentially lead to central nervous system (CNS) side effects of drugs, which normally do not distribute to the brain. However, whereas ABCB1-mediated DDIs at the BBB have been thoroughly studied in preclinical species, relatively few studies have been performed in humans, which may be due to the challenge of quantifying drug concentrations in human brain. Some studies have used an indirect approach, i.e., by measuring CNS pharmacodynamic effects of ABCB1 substrates as a surrogate parameter of drug concentration in the brain (e.g., respiratory depression caused by loperamide).[9,10]

An approach to directly measure drug concentrations in the human brain is positron emission tomography (PET) imaging with microdoses of carbon-11 or fluorine-18-labeled drugs.[8,11] Previously developed ABCB1 substrate probes for PET imaging, which have been used in humans, are racemic [$^{11}$C]verapamil,[12−14] (*R*)-[$^{11}$C]verapamil,[15−19] and [$^{11}$C]-*N*-desmethyl-loperamide.[20,21] In a seminal study Sasongko and colleagues have shown an approximately 2-fold increase in brain distribution of [$^{11}$C]verapamil in humans, when PET scans were performed during continuous intravenous (iv) infusion of the first generation ABCB1 inhibitor cyclosporine A.[13] Following administration of the potent third-generation ABCB1 inhibitor tariquidar,[22] distribution of (*R*)-[$^{11}$C]verapamil and [$^{11}$C]-*N*-desmethyl-loperamide to the human brain was 2 to 5 times increased as compared with PET scans without tariquidar administration.[18−21] For [$^{11}$C]verapamil and (*R*)-[$^{11}$C]verapamil, increases in brain distribution following ABCB1 inhibition with cyclosporine A and tariquidar, respectively, were markedly smaller in humans than in rodents.[18,23] This may at least partly be explained by lower inhibitor plasma concentrations achieved in human studies as compared with rodent studies[1] and possibly also by different expression levels of ABCB1 at the rodent and human BBB.[24]

We hypothesize that additional factors, which are specific to PET imaging studies, such as brain uptake of radiolabeled metabolites or anesthesia, may have contributed to different effects of ABCB1 inhibition on drug brain distribution in rodents and humans observed in PET studies. The aim of this study was to use small-animal PET to systematically assess the influence of several different factors (see Table 1) on the magnitude of the ABCB1-mediated DDI between tariquidar and (*R*)-[$^{11}$C]-verapamil or [$^{11}$C]-*N*-desmethyl-loperamide at the mouse BBB.

**Table 1. Overview of Investigated Factors and Their Influence on the Magnitude of the Interaction between Tariquidar and (*R*)-[$^{11}$C]Verapamil (VPM) or [$^{11}$C]-*N*-Desmethyl-loperamide (dLOP)[a]**

| | baseline PET scan (without tariquidar) | | PET scan after complete ABCB1 inhibn | |
|---|---|---|---|---|
| factor | VPM | dLOP | VPM | dLOP |
| transport activity of ABCB1 for substrate | + | + | − | − |
| density of ABCB1 at BBB | − | − | − | − |
| metabolism of radiotracer | + | + | + | + |
| cerebral blood flow | − | − | − | + |
| isoflurane anesthesia | − | − | − | + |

[a]+: factor has an influence. −: factor has no influence.

## EXPERIMENTAL SECTION

**Chemicals.** If not stated otherwise, chemicals were purchased from Sigma-Aldrich Chemie GmbH (Schnelldorf, Germany) or Merck (Darmstadt, Germany) and were of at least analytical grade. (*R*)-Norverapamil was obtained from ABX GmbH (Radeberg, Germany) and *N*-isopropyl-*p*-iodoamphetamine hydrochloride from abcr GmbH (Karlsruhe, Germany). *N*-Desmethyl-loperamide and *N*-didesmethyl-loperamide were synthesized according to the literature.[25] Isoflurane was obtained from Abbott Laboratories Ltd. (Maidenhead, U.K.). Tariquidar dimesylate was obtained from Xenova Ltd. (Slough, U.K.). For *in vivo* experiments, tariquidar was freshly dissolved prior to each administration in 2.5% (w/v) aqueous (aq) dextrose solution and injected iv at a volume of 4 mL/kg body weight. For *in vitro* experiments, tariquidar was freshly dissolved in dimethyl sulfoxide (<0.1% in final solution). Racemic [$^{3}$H]verapamil, [$^{3}$H]-*N*-desmethyl-loperamide, and [$^{14}$C]mannitol (specific activity: 2.22−3.14 GBq/$\mu$mol, 2.96−3.22 GBq/$\mu$mol, and 1.85−2.22 kBq/$\mu$mol, respectively) were obtained from Hartmann Analytic GmbH (Braunschweig, Germany).

**Cell Lines.** LLC-PK1 cells transduced with human *MDR1* (LLC-ABCB1) or murine *Mdr1a* (LLC-Abcb1a) were kindly provided by Prof. P. Borst and Dr. A. Schinkel (The Netherlands Cancer Institute, Amsterdam, The Netherlands). Culturing of the cells and testing of vincristine sulfate resistance (0.64 $\mu$M) were performed as described earlier.[26]

**Animals.** For the imaging experiments female C57BL/6N wild-type mice (Taconic, Skensved, Denmark) and female homozygous *Abcb1a/1b*$^{(-/-)}$ and heterozygous *Abcb1a/1b*$^{(+/-)}$ mice backcrossed to the C57BL/6 background ($N$ > 10) were used. For the other experiments female wild-type FVB/N mice (Charles River, Sulzfeld, Germany) and female *Abcb1a/1b*$^{(-/-)}$ mice with an FVB genetic background (Taconic, Germantown, NY, USA) were used. All animals were housed in groups under individual ventilated cage conditions in polysulfon type III cages. The environmental conditions were as follows: temperature, 22 ± 3 °C; humidity, 40% to 70%; and a 12-h light/dark cycle (lights on at 6:00) with free access to standard laboratory rodent diet (ssniff R/M-H, ssniff Spezialdiäten GmbH, Soest, Germany) and tap water. An acclimatization period of at least 1 week was allowed before the animals were used in the experiments. All animal experiments were approved by the national authorities (Amt der Niederösterreichischen Landesregierung), and all study procedures were performed in accordance with the European Communities Council Directive of September 22, 2010 (2010/63/EU). All efforts were made to comply with the 3Rs principle in this study.

***In Vitro* Transport Assays.** Bidirectional transport experiments were performed as described earlier.[27] Briefly, cells were seeded with a density of 0.3 × 10$^6$ cells/cm$^2$ on transparent



DOI: 10.1021/acs.molpharmaceut.5b00168
*Mol. Pharmaceutics* 2015, 12, 3214−3225

polyester membrane filters (Transwell-Clear, 6-well, 24 mm diameter, 0.4 $\mu$m pore size, Corning Costar Corporation, Cambridge, MA, USA). 5−7 days after the cells reached 100% confluence, the experiment was initiated with 1 h preincubation, for which culture medium was replaced by serum-free Opti-MEM (Gibco/Life Technologies GmbH, Darmstadt, Germany) without or with tariquidar (5, 10, 20, 35, 50, 200, 500 nM). At the beginning of the experiment, [$^3$H]verapamil or [$^3$H]-*N*-desmethyl-loperamide (both 5 nM) in fresh Opti-MEM was added to either the apical or the basolateral compartment of the Transwell filter. Tariquidar or solvent was added to both compartments. Samples were taken after 60, 120, 240, and 360 min from the chamber opposite where the substrate was added, and the amount of [$^3$H]verapamil or [$^3$H]-*N*-desmethyl-loperamide was quantified with a $\beta$-scintillation counter (Microbeta Trilux, PerkinElmer, Rodgau, Germany). To determine membrane integrity, transepithelial electrical resistance (TEER) and, in representative wells, [$^{14}$C]mannitol diffusion were measured with criteria for exclusion described earlier.[27]

**Analysis of *in Vitro* Transport Data.** Apparent substrate permeability ($P_{app}$) from the basolateral to the apical compartment (b−A) and *vice versa* (a−B) was calculated using the following equation:

$$P_{app}[\mathrm{nm/s}] = (\mathrm{d}Q/\mathrm{d}t)/(AC_0 \times 60)$$

where d$Q$/d$t$ (disintegration/min) is the permeability rate of the substrate into the sample compartment, $A$ the growth area of the monolayer, and $C_0$ the initial substrate concentration in the donor compartment. The transport ratio (TR) was calculated by dividing $P_{app}$(b−A) by $P_{app}$(a−B). A TR > 2 is generally considered as an indicator of active, asymmetrical transport.[28] Normalized response to ABCB1 inhibition was obtained by subtracting the mean TR without tariquidar from the individual TR values with different tariquidar concentrations followed by normalization to the mean TR with maximum ABCB1 inhibition (500 nM tariquidar). With Prism6 software (GraphPad Software, La Jolla, CA, USA) a sigmoidal model with variable slope was used to analyze concentration−response relationships by nonlinear regression.

**Radiotracer Synthesis and Formulation.** (*R*)-[$^{11}$C]-Verapamil and [$^{11}$C]-*N*-desmethyl-loperamide were synthesized by [$^{11}$C]methylation of (*R*)-norverapamil and *N*-didesmethyl-loperamide, respectively, as described in the literature.[25,29] Both radiotracers were formulated for iv injection in physiological saline solution (0.9%, w/v) containing 1% (v/v) Tween 80 at an approximate concentration of 370 MBq/mL. Specific activity at the end of synthesis was 137 ± 34 GBq/$\mu$mol for (*R*)-[$^{11}$C]verapamil and 138 ± 87 GBq/$\mu$mol for [$^{11}$C]-*N*-desmethyl-loperamide. Radiochemical purity of both radiotracers was >98%. *N*-Isopropyl-*p*-[$^{125}$I]iodoamphetamine was synthesized by iodine exchange labeling of *N*-isopropyl-*p*-iodoamphetamine free base with [$^{125}$I]sodium iodide.[30] *N*-Isopropyl-*p*-[$^{125}$I]-iodoamphetamine was obtained with a radiochemical purity >95% and formulated for iv injection in sodium acetate buffered physiological saline solution (0.9%, w/v) at an approximate concentration of 25 MBq/mL.

**PET/MR Imaging.** Groups of female C57BL/6N mice (age 14−16 weeks; body weight 21.2 ± 1.4 g), homozygous *Abcb1a/1b*$^{(-/-)}$ mice (age 11−22 weeks; body weight 21.1 ± 0.9 g), and heterozygous *Abcb1a/1b*$^{(+/-)}$ mice (age 11−17 weeks; body weight 23.6 ± 1.5 g) were either iv injected with vehicle solution (2.5% (w/v) aq dextrose solution) or 1.5, 3, 6, 8, 10, 15, 20, 30 mg/kg body weight tariquidar at 2 h before start of PET imaging ($n$ = 2−6 per group). For injection, mice were preanesthetized in an induction chamber using isoflurane (2.5−3.5% in oxygen) and placed on a heated animal bed (38 °C), and the lateral tail vein was cannulated. Animal respiratory rate and body temperature were constantly monitored (SA Instruments Inc., Stony Brook, NY, USA), and the isoflurane level was adjusted (1.5−2% in oxygen) to achieve a constant and sufficient depth of anesthesia. Anesthesia was maintained for the whole pretreatment and imaging period. Following administration, anatomical magnetic resonance imaging (MRI) was performed on a 1 T benchtop MRI (ICON, Bruker BioSpin GmbH, Ettlingen, Germany) using a modified 3D $T_1$-weighted gradient echo sequence (T1-FLASH) and the following imaging parameters: echo time (TE) = 4.7 ms; repetition time (TR) = 27 ms; flip angle (FA) = 25°; field of view (FOV) = 7.6 × 2.6 × 2.4 cm; matrix = 380 × 130; 32 slices; slice thickness = 750 $\mu$m; total imaging time = 22 min. Following MRI, the animal bed was transferred into the gantry of a microPET scanner (Focus 220, Siemens Medical Solutions, Knoxville, TN, USA), and a 10 min transmission scan using a $^{57}$Co point source was recorded. Subsequently, at 2 h after tariquidar or vehicle injection, either (*R*)-[$^{11}$C]verapamil (32 ± 9 MBq, <0.5 nmol, 0.1 mL, $n$ = 33) or [$^{11}$C]-*N*-desmethyl-loperamide (33 ± 7 MBq, <0.5 nmol, 0.1 mL, $n$ = 38) was administered as an iv bolus over 1 min, and a 60 min dynamic PET scan (energy window, 250−750 keV; timing window, 6 ns) was initiated at the start of radiotracer injection.

**Postimaging Procedures.** After completion of the imaging procedure, a terminal blood sample was withdrawn under isoflurane anesthesia from the retro-orbital sinus vein, and the animals were sacrificed by cervical dislocation. Blood was centrifuged (17000*g*, 4 °C, 4 min) to obtain plasma, and whole brains were removed. Aliquots of blood and plasma as well as whole brains were transferred into preweighed tubes and measured for radioactivity in a gamma counter (Wizard 1470, PerkinElmer, Wellesley, MA, USA). The measured radioactivity data were corrected for radioactive decay and expressed as standardized uptake value ((radioactivity per g/injected radioactivity) × body weight). The remainder of the plasma samples was stored at −80 °C until measurement of tariquidar plasma concentrations using a previously described combined liquid chromatography tandem mass spectrometry (LC/MS) assay.[17]

**PET Data Analysis.** The 60 min dynamic emission PET data were sorted into 23 frames, which incrementally increased in time length from 5 s to 10 min. Images were reconstructed using Fourier rebinning of the 3D sonograms followed by two-dimensional filtered back projection with a ramp filter, resulting in an image voxel size of 0.4 × 0.4 × 0.796 mm$^3$. A standard data correction protocol (normalization, attenuation, and decay correction) was applied to the PET data. The PET units were converted into units of radioactivity concentration by applying a calibration factor derived from imaging of a cylindrical phantom with a known $^{11}$C-radioactivity concentration. Using the image analysis software Amide,[31] whole brain was manually outlined on the PET images, and time−activity curves, expressed in standardized uptake value, were derived. Individual brain-to-blood concentration ratios ($K_{b,brain}$) were calculated by dividing the brain radioactivity concentration in the last PET frame (50 to 60 min after radiotracer injection) by the corresponding blood radioactivity concentration as determined by the gamma counter measurements.

**Analysis of Concentration−Response Relationships.** Normalized response was obtained by subtracting the mean $K_{b,brain}$ value of vehicle treated animals (= no ABCB1 inhibition)


DOI: 10.1021/acs.molpharmaceut.5b00168
*Mol. Pharmaceutics* 2015, 12, 3214−3225

from the individual $K_{b,brain}$ values measured after different tariquidar doses and subsequent normalization to the mean $K_{b,brain}$ value derived from homozygous *Abcb1a/1b*$^{(-/-)}$ mice (= maximum ABCB1 inhibition). Concentration−response relationships were analyzed by nonlinear regression analysis based on a sigmoidal model with variable slope using Prism 6 software.

**Metabolite Analysis.** To investigate the effect of isoflurane anesthesia on metabolism of (*R*)-[$^{11}$C]verapamil and [$^{11}$C]-*N*-desmethyl-loperamide, female wild-type FVB/N mice (age 11−12 weeks; body weight 23.6 ± 1.1 g) were randomly assigned to two cohorts. In one cohort, all procedures were performed in isoflurane anesthetized (1.5−2% in oxygen) animals resulting in a total anesthesia length of 160 min (= long anesthesia). In the second cohort, pretreatment and radiotracer injection were performed in awake animals which were only shortly anesthetized prior to retro-orbital blood sampling, resulting in a total anesthesia length of 5 min (= short anesthesia). All animals were pretreated either with vehicle solution (2.5% (w/v) aq dextrose solution) or with tariquidar at a dose of 15 mg/kg. Two hours after pretreatment, animals received either (*R*)-[$^{11}$C]verapamil (30 ± 3 MBq, <0.5 nmol, 0.1 mL, $n$ = 13) or [$^{11}$C]-*N*-desmethyl-loperamide (40 ± 18 MBq, <0.5 nmol, 0.1 mL, $n$ = 13), and a terminal blood sample was withdrawn at 25 min after radiotracer injection. Blood was centrifuged to obtain plasma, and whole brains were removed. To plasma and homogenized brain tissue were added unlabeled verapamil (10 mg/mL in water, 100 μL) or *N*-desmethyl-loperamide (10 mg/mL in water/acetonitrile; 1/1, v/v, 100 μL), and proteins were precipitated by the addition of acetonitrile (1 μL per μL of plasma and 0.5 mL per brain). The homogenates were vortexed and then centrifuged (12000*g*, 5 min, 21 °C). Each supernatant (plasma, brain, 3 μL each) and diluted radiotracer solution as reference were spotted on thin-layer chromatography (TLC) plates (silica gel 60F 254 nm, 20 × 20 cm; Merck, Darmstadt, Germany), and plates were developed in ethyl acetate/triethylamine (9/1, v/v). Detection was performed by placing the TLC plates on multisensitive phosphor screens (PerkinElmer Life Sciences, Waltham, MA). The screens were scanned at 300 dpi resolution using a PerkinElmer Cyclone Plus Phosphor Imager (PerkinElmer Life Sciences).

**Radiotracer Brain Distribution in Anesthetized/Nonanesthetized Mice.** Brain uptake of (*R*)-[$^{11}$C]verapamil and [$^{11}$C]-*N*-desmethyl-loperamide was assessed in isoflurane anesthetized or awake female wild-type FVB/N mice (age 9−10 weeks; body weight 23.7 ± 4.7 g) or female *Abcb1a/1b*$^{(-/-)}$ mice with an FVB genetic background (age 8−10 weeks; body weight 21.7 ± 5.1 g). Groups of mice were kept for 40 min in an induction chamber flushed with either isoflurane (1.5−2% in oxygen) or room air alone, followed by iv injection of either (*R*)-[$^{11}$C]verapamil (30 ± 12 MBq, <0.5 nmol, 0.1 mL, $n$ = 16), [$^{11}$C]-*N*-desmethyl-loperamide (19 ± 5 MBq, <0.5 nmol, 0.1 mL, $n$ = 18), or *N*-isopropyl-*p*-[$^{125}$I]iodoamphetamine (2 ± 0.5 MBq, 0.1 mL, $n$ = 8). Mice were sacrificed by cervical dislocation at 5 min (*N*-isopropyl-*p*-[$^{125}$I]iodoamphetamine) or 25 min ((*R*)-[$^{11}$C]verapamil and [$^{11}$C]-*N*-desmethyl-loperamide) after injection, blood was collected by cardiac puncture, and whole brains were removed. Blood and brain were transferred to preweighed tubes and measured for radioactivity in a gamma counter. The measured radioactivity data were corrected for radioactive decay, and $K_{b,brain}$ values were calculated.

**Plasma Protein Binding.** Plasma protein binding of (*R*)-[$^{11}$C]verapamil and [$^{11}$C]-*N*-desmethyl-loperamide was determined in triplicate by adding radiotracer solution (3 μL, 0.4 MBq) to C57BL/6N mouse plasma (without and with addition of tariquidar in 2.5% dextrose solution, final concentration: 2400 nM) or human plasma (600 μL), both collected in heparinized tubes, followed by 20 min incubation at 37 °C. In order to avoid adsorption of radiotracers to the filter membrane, Amicon Ultra 0.5 mL filters (Millipore Corporation, Bedford, MA, USA) were preconditioned by adding a solution of unlabeled verapamil or *N*-desmethyl-loperamide (10 mg/mL, 200 μL) followed by centrifugation (12000*g*, 10 min, 25 °C). After incubation, plasma aliquots (200 μL) were transferred to the preconditioned Amicon filters, which were centrifuged (12000*g*, 30 min, 25 °C). Filters and tubes were separately measured in a gamma counter, and the obtained data were decay corrected. Percent plasma protein binding was calculated as percent radioactivity in the filter relative to total radioactivity (filter and tube).

**Statistical Analysis.** Statistical differences between two groups were analyzed with two-tailed *t*-tests and between multiple groups with one-way analysis of variance (ANOVA) followed by Bonferroni's multiple comparison test using Prism6 software, and $P$ values of <0.05 were considered significant. If not stated otherwise, all values are presented as mean ± standard deviation (SD).

## RESULTS

***In Vitro* Transport of [$^{3}$H]Verapamil and [$^{3}$H]-*N*-Desmethyl-loperamide in ABCB1 and Abcb1a Overexpressing LLC Monolayers and Transport Inhibition by Tariquidar.** Transcellular transport of [$^{3}$H]verapamil and [$^{3}$H]-*N*-desmethyl-loperamide was assessed in the basolateral to apical (b−A) and apical to basolateral (a−B) direction across monolayers of LLC cells overexpressing either ABCB1 or Abcb1a (Figure 1). For both compounds, basolateral-to-apical transport was greater than apical-to-basolateral transport (Figures 1A and 1B), indicating asymmetrical ABCB1/Abcb1a-mediated transport. The basolateral-to-apical to apical-to-basolateral transport ratios (TR) were for each substrate similar in ABCB1- and Abcb1a-transfected cells (Figures 1A and 1B). TR of [$^{3}$H]-*N*-desmethyl-loperamide was 5 times higher than TR of [$^{3}$H]-verapamil in ABCB1-transfected cells (18.5 ± 1.7 vs 3.7 ± 0.4, $P$ < 0.001) and 8.6 times higher than TR of [$^{3}$H]verapamil in Abcb1a-transfected cells (27.6 ± 6.5 vs 3.2 ± 0.4, $P$ < 0.001). In LLC wild-type cells TRs were 1.2 ± 0.1 for [$^{3}$H]verapamil and 1.6 ± 0.03 for [$^{3}$H]-*N*-desmethyl-loperamide (data not shown). [$^{3}$H]Verapamil and [$^{3}$H]-*N*-desmethyl-loperamide transport was also assessed in the presence of increasing tariquidar concentrations and concentration−response curves fitted to the data (Figures 1C and 1D). Estimated $IC_{50}$ values of tariquidar were for both substrates comparable in ABCB1- and Abcb1a-transfected cells ([$^{3}$H]verapamil, ABCB1 17.2 nM, Abcb1a 17.9 nM; [$^{3}$H]-*N*-desmethyl-loperamide, ABCB1 9.0 nM, Abcb1a 6.0 nM).

***In Vivo* Brain Distribution of (*R*)-[$^{11}$C]Verapamil and [$^{11}$C]-*N*-Desmethyl-loperamide in C57BL/6N Wild-Type, Homozygous *Abcb1a/1b*$^{(-/-)}$, and Heterozygous *Abcb1a/1b*$^{(+/-)}$ Mice and Tariquidar Concentration−Response Relationship.** Brain distribution of (*R*)-[$^{11}$C]verapamil and [$^{11}$C]-*N*-desmethyl-loperamide was studied with PET in C57BL/6N wild-type mice treated with either vehicle or escalating tariquidar doses (Figures 2 and 3). Brain time−activity curves of (*R*)-[$^{11}$C]verapamil and [$^{11}$C]-*N*-desmethyl-loperamide had a different shape. Following injection, radioactivity in the brain reached an approximately 3−4 times higher peak concentration


DOI: 10.1021/acs.molpharmaceut.5b00168
*Mol. Pharmaceutics* 2015, 12, 3214−3225

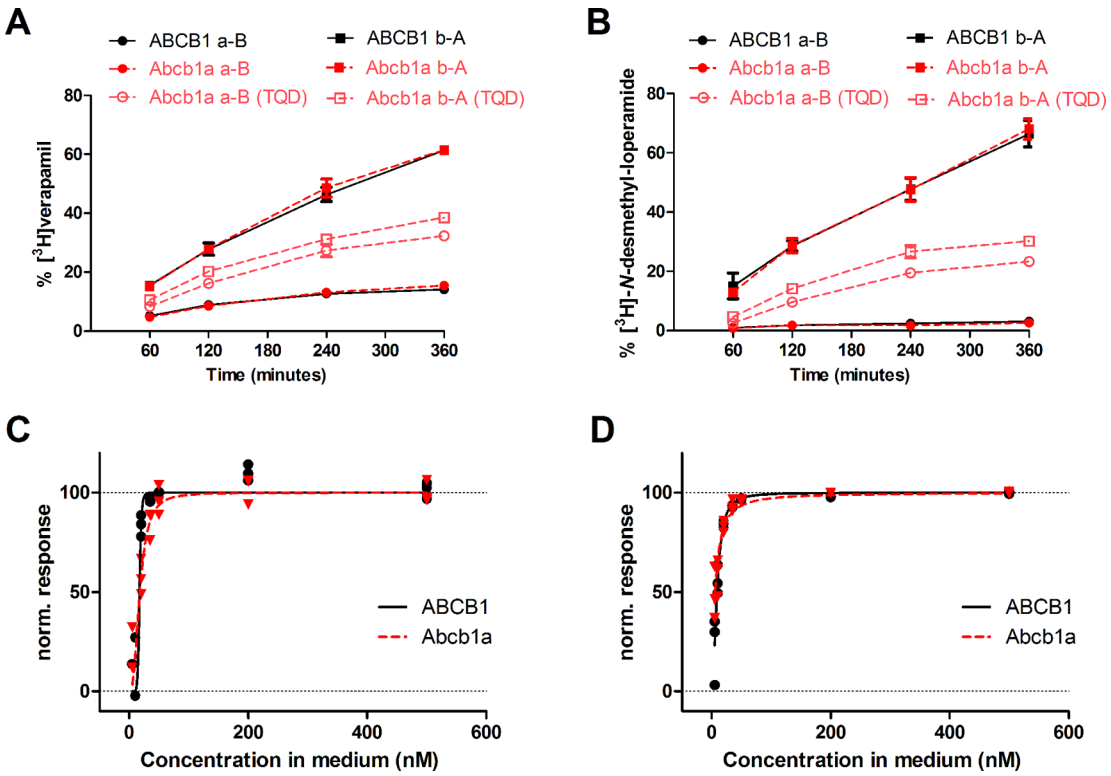


**Figure 1.** Bidirectional transport of [$^3$H]verapamil (A) and [$^3$H]-*N*-desmethyl-loperamide (B) by ABCB1- (black) and Abcb1a-transfected LLC cells (red) shown as % of initial concentration in the donor compartment over 360 min without tariquidar. For Abcb1a-transfected LLC cells, transport of [$^3$H]verapamil and [$^3$H]-*N*-desmethyl-loperamide is also shown in the presence of 500 nM tariquidar (TQD, open red symbols). All experiments were performed in triplicate, and values are shown as mean ± SD. The normalized response to ABCB1 inhibition of [$^3$H]verapamil (C) and [$^3$H]-*N*-desmethyl-loperamide (D) transport in ABCB1- (black) and Abcb1a-transfected cells (red) was calculated based on transport ratios (TR) over 6 h in bidirectional transport assays (see Experimental Section) and is plotted against tariquidar concentration (nM) in the assay medium. A sigmoidal Hill function was fitted to the data and gave for transport of [$^3$H]verapamil an estimated half-maximum inhibitory concentration ($IC_{50}$) of 17.2 nM (95% confidence interval CI: 6.7−44.3) and a Hill slope of 10.8 (95% CI: −56.3 to 77.8) for ABCB1-transfected cells, and an $IC_{50}$ of 17.9 nM (95% CI: 14.1−22.6) and a Hill slope of 2.6 (95% CI: 1.1−4.2) for Abcb1a-transfected cells (C). For transport of [$^3$H]-*N*-desmethyl-loperamide an $IC_{50}$ of 9.0 nM (95% CI: 8.1−10.0) and a Hill slope of 2.1 (95% CI: 1.6−2.5) was estimated for ABCB1-transfected cells, and for Abcb1a-transfected cells an $IC_{50}$ of 6.0 nM (95% CI: 4.9−7.3) and a Hill slope of 1.3 (95% CI: 0.9−1.6) (D). For definition of normalized response refer to the Experimental Section.

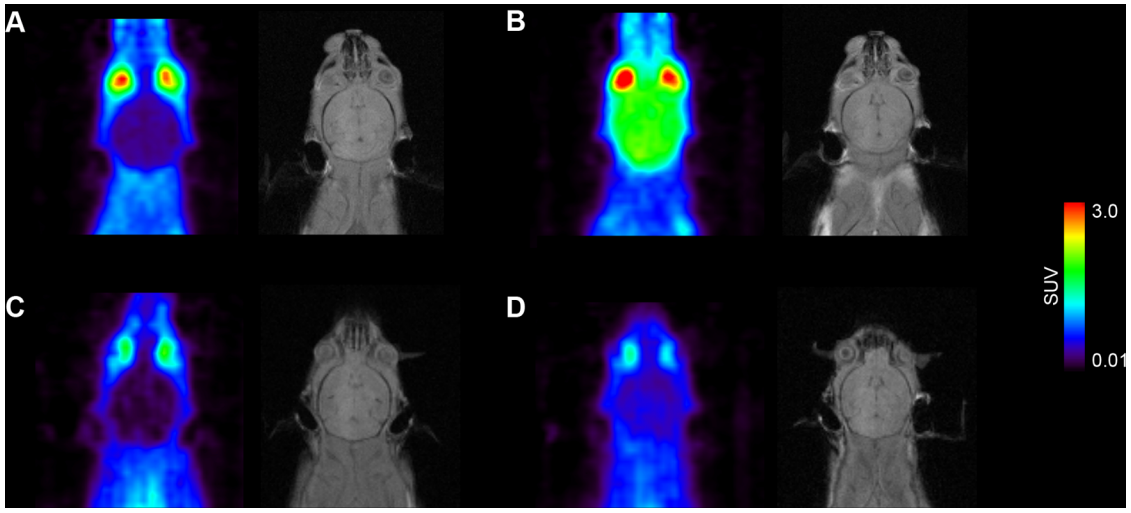


**Figure 2.** Coronal positron emission tomography (PET) summation images (0 to 60 min) and corresponding planes of $T_1$-weighted gradient echo MR images of the brain region obtained after iv injection of (*R*)-[$^{11}$C]verapamil (A, B) and [$^{11}$C]-*N*-desmethyl-loperamide (C, D) in vehicle treated (left panel) or tariquidar treated (15 mg/kg, at 2 h before PET) (right panel) C57BL/6N wild-type mice. Radiation scale is set from 0.01 to 3.0 standardized uptake value (SUV).

for (*R*)-[$^{11}$C]verapamil than for [$^{11}$C]-*N*-desmethyl-loperamide, which was followed by washout of radioactivity (Figure 3A). For [$^{11}$C]-*N*-desmethyl-loperamide, radioactivity in the brain stayed on the same level after peak concentration with only minimal washout, which was consistent with lysosomal trapping of [$^{11}$C]-*N*-desmethyl-loperamide in brain parenchyma (Figure 3B).



DOI: 10.1021/acs.molpharmaceut.5b00168
*Mol. Pharmaceutics* 2015, 12, 3214−3225

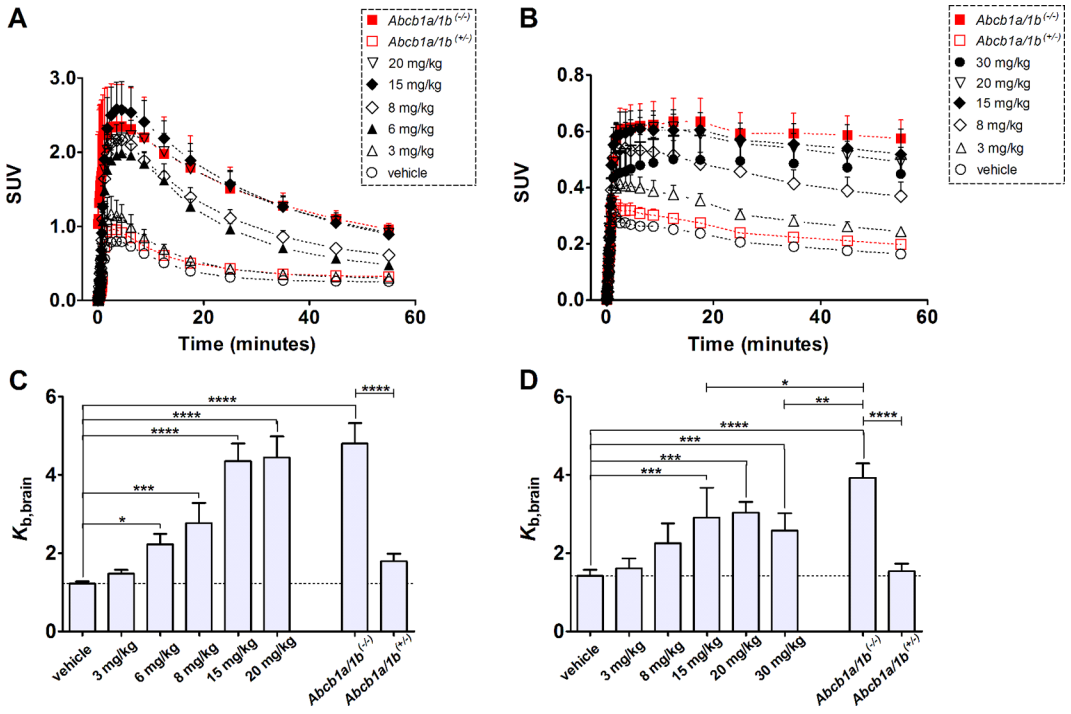


**Figure 3.** Mean (+ SD, $n = 3–6$ per dose group) whole brain time−activity curves of (*R*)-[$^{11}$C]verapamil (A) and [$^{11}$C]-*N*-desmethyl-loperamide (B) in C57BL/6N wild-type mice treated with different doses of tariquidar or vehicle at 2 h before start of the PET scan (black symbols) and in homozygous *Abcb1a/1b*$^{(-/-)}$ and heterozygous *Abcb1a/1b*$^{(+/-)}$ mice treated with vehicle (red symbols). Lower panels show the mean (+ SD) brain-to-blood concentration ratios at the end of the PET scan ($K_{b,brain}$) for (*R*)-[$^{11}$C]verapamil (C) and [$^{11}$C]-*N*-desmethyl-loperamide (D) after treatment with vehicle or different tariquidar doses. In addition, $K_{b,brain}$ values in vehicle treated homozygous *Abcb1a/1b*$^{(-/-)}$ and heterozygous *Abcb1a/1b*$^{(+/-)}$ mice are shown in panels C and D. The dotted line indicates mean $K_{b,brain}$ of vehicle treated wild-type mice. Statistical differences are indicated by asterisks (*, $P < 0.05$; **, $P < 0.01$; ***, $P < 0.001$; ****, $P < 0.0001$, one-way ANOVA with Bonferroni's multiple comparison test).

Brain uptake of (*R*)-[$^{11}$C]verapamil and [$^{11}$C]-*N*-desmethyl-loperamide was expressed as the brain-to-blood concentration ratio ($K_{b,brain}$), which was calculated by dividing the radioactivity concentration measured in the last PET time frame (50 to 60 min after radiotracer injection) by the radioactivity concentration measured in blood at the end of the PET scan (Figures 3C and 3D). Blood radioactivity concentrations of (*R*)-[$^{11}$C]verapamil were unchanged after tariquidar pretreatment. In contrast, blood radioactivity concentrations of [$^{11}$C]-*N*-desmethyl-loperamide were increased in tariquidar treated compared to vehicle treated mice (see Supporting Information). $K_{b,brain}$ values in vehicle treated wild-type mice were 1.22 ± 0.06 for (*R*)-[$^{11}$C]verapamil and 1.42 ± 0.16 for [$^{11}$C]-*N*-desmethyl-loperamide. Pretreatment of wild-type mice with escalating doses of tariquidar (1.5, 3, 6, 8, 10, 15, 20, and 30 mg/kg body weight) led to a dose dependent increase in $K_{b,brain}$ for both radiotracers, resulting in a $K_{b,brain}$ of 4.44 ± 0.54 for (*R*)-[$^{11}$C]verapamil (after 20 mg/kg tariquidar) and 2.58 ± 0.44 for [$^{11}$C]-*N*-desmethyl-loperamide (after 30 mg/kg tariquidar) (Figures 3C and 3D). Tariquidar plasma concentrations, determined at the end of the PET scan, were 158 ± 7 nM (range: 153−163 nM) for the lowest (1.5 mg/kg) and 3508 ± 427 nM (range: 2802−3863 nM) for the highest administered dose (30 mg/kg). $K_{b,brain}$ in vehicle treated homozygous *Abcb1a/1b*$^{(-/-)}$ mice was 4.81 ± 0.51 for (*R*)-[$^{11}$C]-verapamil and 3.93 ± 0.36 for [$^{11}$C]-*N*-desmethyl-loperamide, which corresponded to 3.9-fold and 2.8-fold increases over vehicle treated wild-type mice ($P < 0.0001$), respectively. In heterozygous *Abcb1a/1b*$^{(+/-)}$ mice, mean $K_{b,brain}$ values were only minimally and not significantly increased when compared to vehicle treated wild-type mice ((*R*)-[$^{11}$C]verapamil, $K_{b,brain}$ 1.79 ± 0.19, 1.5-fold increase; [$^{11}$C]-*N*-desmethyl-loperamide, $K_{b,brain}$ 1.54 ± 0.19, 1.1-fold increase) (Figures 3C and 3D).

$K_{b,brain}$ values of (*R*)-[$^{11}$C]verapamil and [$^{11}$C]-*N*-desmethyl-loperamide in tariquidar treated wild-type mice were normalized to $K_{b,brain}$ values in *Abcb1a/1b*$^{(-/-)}$ mice and plotted against tariquidar plasma concentrations, and sigmoidal Hill curves were fitted to the data (Figure 4). The estimated $IC_{50}$ values of tariquidar were similar for (*R*)-[$^{11}$C]verapamil (1052 nM, 95% confidence interval, CI: 930−1189 nM) and [$^{11}$C]-*N*-desmethyl-loperamide (1329 nM, 95% CI: 980−1801 nM).

**Plasma and Brain Metabolites of (*R*)-[$^{11}$C]Verapamil and [$^{11}$C]-*N*-Desmethyl-loperamide in Vehicle and Tariquidar Treated Wild-Type FVB/N Mice.** Radiolabeled metabolites in plasma and brain were determined for both radiotracers in groups of vehicle treated or tariquidar treated wild-type FVB/N mice at 25 min after radiotracer injection (Table 2). Radiolabeled metabolites were first examined in isoflurane anesthetized mice subjected to a comparable anesthesia duration as for the *in vivo* imaging experiments (160 min = long anesthesia). For both radiotracers radiolabeled metabolites were detected in plasma, with less intact radiotracer for [$^{11}$C]-*N*-desmethyl-loperamide than for (*R*)-[$^{11}$C]verapamil (Table 2). For both radiotracers, radiolabeled metabolites were also detected in brain. In tariquidar treated mice the percentage of intact radiotracer in brain was for both radiotracers higher than in vehicle treated mice (Table 2).

**Influence of Isoflurane Anesthesia on Metabolism of (*R*)-[$^{11}$C]Verapamil and [$^{11}$C]-*N*-Desmethyl-loperamide.** The influence of isoflurane anesthesia on plasma and brain metabolites of (*R*)-[$^{11}$C]verapamil and [$^{11}$C]-*N*-desmethyl-loperamide was determined in additional groups of awake mice, which were


DOI: 10.1021/acs.molpharmaceut.5b00168
*Mol. Pharmaceutics* 2015, 12, 3214−3225

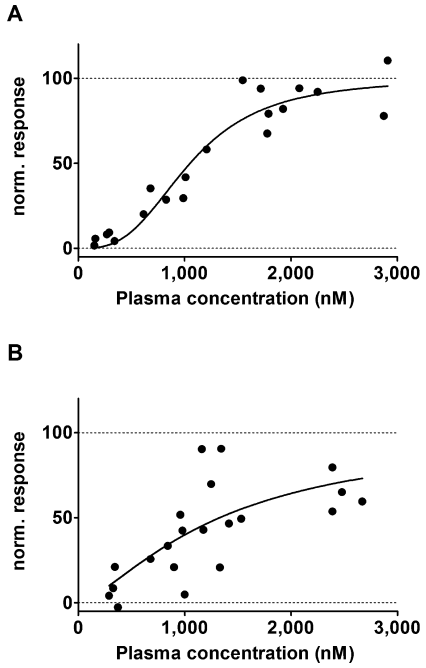


**Figure 4.** Normalized response in terms of increase in brain-to-blood concentration ratio at the end of the PET scan ($K_{b,brain}$) for (*R*)-[$^{11}$C]verapamil (A) and [$^{11}$C]-*N*-desmethyl-loperamide (B) in C57BL/6N wild-type mice plotted against tariquidar plasma concentration (nM) measured at the end of the PET scan. For [$^{11}$C]-*N*-desmethyl-loperamide, data after 30 mg/kg tariquidar were excluded. A sigmoidal Hill function was fitted to the data and gave an estimated half-maximum inhibitory concentration ($IC_{50}$) of 1052 nM (95% confidence interval CI: 930−1189) and a Hill slope of 2.98 (95% CI: 2.00−3.95) for (*R*)-[$^{11}$C]verapamil (A) and an $IC_{50}$ of 1329 nM (95% CI: 980−1801) and a Hill slope of 1.44 (95% CI: 0.50−2.38) for [$^{11}$C]-*N*-desmethyl-loperamide (B). Goodness of fit ($R^2$) was 0.919 for (*R*)-[$^{11}$C]verapamil and 0.508 for [$^{11}$C]-*N*-desmethyl-loperamide. For definition of normalized response refer to the Experimental Section.

**Table 2. Metabolism of (*R*)-[$^{11}$C]Verapamil and [$^{11}$C]-*N*-Desmethyl-loperamide**[a]

| | long anesthesia (160 min) | | short anesthesia (5 min) | |
|---|---|---|---|---|
| | vehicle | tariquidar 15 mg/kg | vehicle | tariquidar 15 mg/kg |
| | (*R*)-[$^{11}$C]Verapamil | | | |
| *n* | 4 | 5 | 4 | |
| plasma | 47 ± 6 | 37 ± 8 | 45 ± 8 | nd |
| brain | 43 ± 22 | 89 ± 2 | 39 ± 26 | nd |
| | [$^{11}$C]-*N*-Desmethyl-loperamide | | | |
| *n* | 3 | 3 | 4 | 3 |
| plasma | 13 ± 4 | 7 ± 1 | 22 ± 2[c] | 18 ± 1[d] |
| brain | 28 ± 13 | 77 ± 6 | 53 ± 13[b] | 70 ± 11 |

[a]Percentage of unchanged (*R*)-[$^{11}$C]verapamil and [$^{11}$C]-*N*-desmethyl-loperamide in plasma and brain of vehicle treated and tariquidar treated (15 mg/kg) wild-type FVB/N mice, determined at 25 min after radiotracer injection under long (160 min) and short (5 min) isoflurane anesthesia. All data are given as mean ± SD; nd = not determined. [b]$P < 0.05$ when compared to corresponding long anesthesia group (2-tailed *t*-test). [c]$P < 0.01$ when compared to corresponding long anesthesia group (2-tailed *t*-test). [d]$P \leq 0.001$ when compared to corresponding long anesthesia group (2-tailed *t*-test).

only shortly anesthetized immediately before retro-orbital blood sampling at the end of the experimental period (5 min anesthesia duration = short anesthesia). For (*R*)-[$^{11}$C]verapamil, the percentage of unchanged parent in plasma and brain of vehicle treated mice was not significantly different from that for mice under long anesthesia (Table 2). For [$^{11}$C]-*N*-desmethyl-loperamide, the percentage of unchanged parent in plasma was significantly higher in vehicle treated mice under short than under long anesthesia (22 ± 2% vs 13% ± 4%, respectively, $P = 0.01$) (Table 2). Radiolabeled metabolites of [$^{11}$C]-*N*-desmethyl-loperamide were further determined in tariquidar treated mice under short anesthesia. Similar to vehicle treated mice, the percentage of unchanged [$^{11}$C]-*N*-desmethyl-loperamide in tariquidar treated mice was significantly higher in animals under short than in animals under long anesthesia (18 ± 1% vs 7 ± 1%, respectively, $P = 0.001$).

**Influence of Isoflurane Anesthesia on Brain Distribution of (*R*)-[$^{11}$C]Verapamil and [$^{11}$C]-*N*-Desmethyl-loperamide.** Brain distribution of (*R*)-[$^{11}$C]verapamil and [$^{11}$C]-*N*-desmethyl-loperamide was compared at 25 min after radiotracer injection in groups of long anesthetized (160 min) and short anesthetized (5 min) mice, treated with either vehicle or tariquidar (15 mg/kg) (Table 3). For (*R*)-[$^{11}$C]verapamil, $K_{b,brain}$ values were not significantly different between long and short anesthetized, vehicle treated mice. Tariquidar pretreatment resulted in a 5.1-fold increase of (*R*)-[$^{11}$C]verapamil $K_{b,brain}$ relative to vehicle group in long anesthetized mice. $K_{p,brain}$ values corrected for the percentages of unchanged (*R*)-[$^{11}$C]verapamil in brain and plasma ($K_{p,brain,VPM}$) showed a 14.1-fold increase in tariquidar treated relative to vehicle treated mice under long anesthesia. In vehicle treated, short anesthetized mice, $K_{p,brain,VPM}$ was not significantly different compared to vehicle treated long anesthetized mice.

For [$^{11}$C]-*N*-desmethyl-loperamide $K_{b,brain}$ values were comparable between vehicle treated long and short anesthetized mice but significantly different between tariquidar treated long and short anesthetized mice (0.93 ± 0.01 vs, 1.57 ± 0.10, $P = 0.0001$). Also $K_{p,brain,dLOP}$ values were not significantly different between vehicle treated long and short anesthetized mice, but significantly different between tariquidar treated long and short anesthetized animals (7.34 ± 0.58 vs 4.85 ± 0.29, $P = 0.01$). Tariquidar induced increase in $K_{p,brain,dLOP}$ values was 18.3-fold for long anesthetized and 9.6-fold for short anesthetized mice (Table 3).

**Influence of Isoflurane Anesthesia on Cerebral Blood Flow.** Cerebral blood flow (CBF) was assessed with *N*-isopropyl-*p*-[$^{125}$I]iodoamphetamine in groups of isoflurane anesthetized and awake mice (Table 4). $K_{b,brain}$ values at 5 min after injection of *N*-isopropyl-*p*-[$^{125}$I]iodoamphetamine were significantly higher in isoflurane anesthetized than in awake mice (12.2 ± 0.4 vs 7.5 ± 0.8, $P < 0.001$) consistent with higher CBF under isoflurane anesthesia (Table 4).

**Influence of CBF on Brain Distribution of (*R*)-[$^{11}$C]-Verapamil and [$^{11}$C]-*N*-Desmethyl-loperamide in Wild-Type FVB/N and *Abcb1a/1b*$^{(-/-)}$ Mice.** The effect of CBF on brain distribution of (*R*)-[$^{11}$C]verapamil and [$^{11}$C]-*N*-desmethyl-loperamide was studied in isoflurane anesthetized and awake wild-type and *Abcb1a/1b*$^{(-/-)}$ mice (Table 4). For (*R*)-[$^{11}$C]verapamil no significant differences in $K_{b,brain}$ were found between anesthetized and awake wild-type or *Abcb1a/1b*$^{(-/-)}$ mice. For [$^{11}$C]-*N*-desmethyl-loperamide, $K_{b,brain}$ values were not significantly different between anesthetized and awake wild-type animals. However, in *Abcb1a/1b*$^{(-/-)}$ mice $K_{b,brain}$ values were significantly lower in anesthetized than in awake animals (1.42 ± 0.40 vs 2.84 ± 0.14, $P < 0.001$). Consequently the $K_{b,brain}$ ratio of *Abcb1a/1b*$^{(-/-)}$ to wild-type mice was for [$^{11}$C]-*N*-desmethyl-loperamide higher in awake than in isoflurane anesthetized mice


DOI: 10.1021/acs.molpharmaceut.5b00168
*Mol. Pharmaceutics* 2015, 12, 3214−3225

**Table 3. Brain-to-Blood ($K_{b,brain}$) and Brain-to-Plasma ($K_{p,brain}$) Concentration Ratios for Total Radioactivity as Well as for Unchanged Parent Tracer ($K_{p,brain,VPM}$ or $K_{p,brain,dLOP}$) in Vehicle Treated and Tariquidar Treated (15 mg/kg) Wild-Type FVB/N Mice Determined at 25 min after Injection of Either (*R*)-[$^{11}$C]Verapamil or [$^{11}$C]-*N*-Desmethyl-loperamide under Long (160 min) and Short (5 min) Isoflurane Anesthesia[a]**

| | long anesthesia (160 min) | | | short anesthesia (5 min) | | |
|---|---|---|---|---|---|---|
| | vehicle | tariquidar 15 mg/kg | fold increase | vehicle | tariquidar 15 mg/kg | fold increase |
| | | | (*R*)-[$^{11}$C]Verapamil | | | |
| *n* | 4 | 3 | | 4 | | |
| $K_{b,brain}$ | 0.44 ± 0.07 | 2.24 ± 0.49 | 5.1 | 0.52 ± 0.07 | nd | nd |
| $K_{p,brain}$ | 0.29 ± 0.04 | 1.53 ± 0.30 | 5.2 | 0.35 ± 0.06 | nd | nd |
| $K_{p,brain,VPM}$ | 0.27 ± 0.12 | 3.83 ± 0.30 | 14.1 | 0.29 ± 0.18 | nd | nd |
| | | | [$^{11}$C]-*N*-Desmethyl-loperamide | | | |
| *n* | 3 | 3 | | 4 | 3 | |
| $K_{b,brain}$ | 0.23 ± 0.04 | 0.93 ± 0.01 | 4.0 | 0.22 ± 0.01 | 1.57 ± 0.10[c] | 7.0 |
| $K_{p,brain}$ | 0.18 ± 0.04 | 0.67 ± 0.01 | 3.7 | 0.20 ± 0.01 | 1.32 ± 0.10[c] | 6.6 |
| $K_{p,brain,dLOP}$ | 0.40 ± 0.16 | 7.34 ± 0.58 | 18.3 | 0.51 ± 0.18 | 4.85 ± 0.29[b] | 9.6 |

[a]All data are given as mean ± SD; nd = not determined. [b]$P < 0.05$ when compared to corresponding long anesthesia group (2-tailed *t*-test). [c]$P < 0.001$ when compared to corresponding long anesthesia group (2-tailed *t*-test).

**Table 4. Effect of Cerebral Blood Flow on Brain-to-Blood ($K_{b,brain}$) and Brain-to-Plasma ($K_{p,brain}$) Concentration Ratios Determined at 25 min after Injection of (*R*)-[$^{11}$C]Verapamil and [$^{11}$C]-*N*-Desmethyl-loperamide in Wild-Type FVB/N and *Abcb1a/1b*$^{(-/-)}$ Mice[a]**

| | isoflurane | | | awake | | |
|---|---|---|---|---|---|---|
| | wild-type | *Abcb1a/1b*$^{(-/-)}$ | fold increase | wild-type | *Abcb1a/1b*$^{(-/-)}$ | fold increase |
| | | | (*R*)-[$^{11}$C]Verapamil | | | |
| *n* | 4 | 4 | | 4 | 4 | |
| $K_{b,brain}$ | 0.49 ± 0.11 | 2.60 ± 0.37 | 5.3 | 0.53 ± 0.04 | 2.77 ± 0.26 | 5.2 |
| $K_{p,brain}$ | 0.35 ± 0.09 | 1.91 ± 0.21 | 5.4 | 0.38 ± 0.03 | 2.15 ± 0.18 | 5.7 |
| | | | [$^{11}$C]-*N*-Desmethyl-loperamide | | | |
| *n* | 3 | 4 | | 5 | 6 | |
| $K_{b,brain}$ | 0.25 ± 0.06 | 1.42 ± 0.4 | 5.7 | 0.21 ± 0.05 | 2.84 ± 0.14[b] | 13.8 |
| $K_{p,brain}$ | 0.20 ± 0.04 | 1.21 ± 0.41 | 6.0 | 0.20 ± 0.05 | 2.79 ± 0.20[b] | 13.7 |
| | | | *N*-Isopropyl-*p*-[$^{125}$I]iodo-amphetamine | | | |
| *n* | 4 | | | 4 | | |
| $K_{b,brain}$ | 12.2 ± 0.4 | nd | nd | 7.5 ± 0.8[b] | nd | nd |

[a]Relative cerebral blood flow was assessed by measurement of $K_{b,brain}$ of *N*-isopropyl-*p*-[$^{125}$I]iodoamphetamine at 5 min after iv injection under otherwise identical experimental conditions. All data are given as mean ± SD; nd = not determined. [b]$P < 0.001$ when compared to corresponding isoflurane group (2-tailed *t*-test).

(13.8 vs 5.7) but similar for (*R*)-[$^{11}$C]verapamil in both groups of animals (Table 4).

**Protein Binding of (*R*)-[$^{11}$C]Verapamil and [$^{11}$C]-*N*-Desmethyl-loperamide in Mouse and Human Plasma.** The percentage of non-protein bound (*R*)-[$^{11}$C]verapamil and [$^{11}$C]-*N*-desmethyl-loperamide in mouse plasma was determined without and with addition of tariquidar at a concentration which was comparable to *in vivo* plasma concentrations (2400 nM) (Table 5). The percentages of non-protein bound (*R*)-[$^{11}$C]verapamil and [$^{11}$C]-*N*-desmethyl-loperamide in mouse plasma were unchanged when tariquidar was added. In human plasma, the percentage of non-protein bound radiotracer was significantly different compared to untreated mouse plasma for (*R*)-[$^{11}$C]verapamil but not for [$^{11}$C]-*N*-desmethyl-loperamide (Table 5).

## DISCUSSION

In this study we used PET to examine at the mouse BBB the interaction between the ABCB1 inhibitor tariquidar and the ABCB1 substrates (*R*)-[$^{11}$C]verapamil and [$^{11}$C]-*N*-desmethyl-loperamide, for which clinical PET data in healthy volunteers are available from the literature.[18−21] We tested the impact of different factors on the magnitude of these ABCB1-mediated DDIs at the mouse BBB (see Table 1) in an attempt to better understand previously observed species differences between rodents and humans.[18] The ABCB1 inhibitor tariquidar has been shown to also inhibit ABCG2, but at higher concentrations than needed for inhibition of ABCB1.[32] However, as (*R*)-[$^{11}$C]verapamil and [$^{11}$C]-*N*-desmethyl-loperamide are not transported by ABCG2 at the BBB,[33,34] we expect that we were selectively looking at the function of ABCB1 at the BBB.

We first performed *in vitro* transport experiments with [$^{3}$H]verapamil and [$^{3}$H]-*N*-desmethyl-loperamide in ABCB1 and Abcb1a overexpressing LLC cells in order to study possible species differences in transport of these two substrates. We used concentrations (5 nM) which were comparable with concentrations achieved *in vivo* in PET experiments when tracer doses of (*R*)-[$^{11}$C]verapamil and [$^{11}$C]-*N*-desmethyl-loperamide are administered. Each substrate had comparable basolateral-to-apical to apical-to-basolateral TRs in ABCB1- and Abcb1a-transfected cells (Figures 1A and 1B). Moreover, $IC_{50}$ values of tariquidar for transport inhibition were for each substrate similar in ABCB1- and Abcb1a-transfected cells (Figures 1C and 1D), which suggested that there were no species differences in


DOI: 10.1021/acs.molpharmaceut.5b00168
*Mol. Pharmaceutics* 2015, 12, 3214−3225

**Table 5. Percentage of Non-Protein Bound (*R*)-[$^{11}$C]Verapamil and [$^{11}$C]-*N*-Desmethyl-loperamide in C57BL/6N Mouse Plasma and Human Plasma without and with Tariquidar (2400 nM)[a]**

| | mouse | | human | |
|---|---|---|---|---|
| | without tariquidar | with tariquidar | without tariquidar | with tariquidar |
| (*R*)-[$^{11}$C]verapamil | 19.9 ± 2.5 | 20.6 ± 2.4 | 15.9 ± 0.5[b] | nd |
| [$^{11}$C]-*N*-desmethyl-loperamide | 14.5 ± 1.8 | 12.0 ± 1.0 | 13.9 ± 0.7 | nd |

[a]All data are given as mean ± SD; nd = not determined. [b]$P < 0.05$, when compared to corresponding mouse group (2-tailed *t*-test).

ABCB1/Abcb1a transport and inhibition. Interestingly, TRs were in both cell types 5 to 9 times higher for [$^{3}$H]-*N*-desmethyl-loperamide (Figure 1B) than for [$^{3}$H]verapamil (Figure 1A), which suggested that the transport activity/rate of ABCB1/Abcb1a is higher for [$^{3}$H]-*N*-desmethyl-loperamide than for [$^{3}$H]verapamil. Higher TRs of [$^{3}$H]-*N*-desmethyl-loperamide observed *in vitro* were consistent with lower *in vivo* brain radioactivity concentrations for [$^{11}$C]-*N*-desmethyl-loperamide than for (*R*)-[$^{11}$C]verapamil (Figure 2), similar to results from studies in humans,[18,20] and with higher increases in metabolite-corrected $K_{p,brain}$ values following tariquidar administration for [$^{11}$C]-*N*-desmethyl-loperamide than for (*R*)-[$^{11}$C]verapamil (see below and Table 3). This suggests that the affinity of a substrate to ABCB1 may determine brain uptake in baseline PET scans without inhibitor administration and thereby influence the magnitude of ABCB1-mediated DDIs.

We next performed (*R*)-[$^{11}$C]verapamil and [$^{11}$C]-*N*-desmethyl-loperamide PET scans in wild-type mice after administration of different tariquidar doses (Figure 3). In previous clinical PET studies kinetic modeling was employed to obtain total distribution volume ($V_T$) as an outcome parameter of radiotracer brain distribution.[18,20] $V_T$ equals the brain-to-plasma concentration ratio at steady state. However, determination of $V_T$ requires arterial blood sampling, which is technically not feasible in mice. We therefore determined brain-to-blood concentration ratios at the end of the PET scan ($K_{b,brain}$) as an estimate of $V_T$. $K_{b,brain}$ values were not determined at steady state and may therefore be variable depending on the time point of measurement after radiotracer injection. However, retrospective analysis of our human PET data showed good correlation between $K_{b,brain}$ and $V_T$ values (see Supporting Information), indicating that $K_{b,brain}$ may be used as a surrogate parameter of $V_T$. Maximum possible brain uptake after complete ABCB1 inhibition was defined in *Abcb1a/1b*$^{(-/-)}$ mice. Both (*R*)-[$^{11}$C]verapamil and [$^{11}$C]-*N*-desmethyl-loperamide showed a tariquidar dose dependent increase in brain distribution (Figure 3), in analogy to previous results in rats and humans.[18−21,35] For (*R*)-[$^{11}$C]verapamil, maximum increase in $K_{b,brain}$ over baseline was 3.6-fold, which was in good agreement with maximum increases observed in humans,[19] but lower than maximum increases observed in rats (10-fold).[35] Interestingly, whereas for (*R*)-[$^{11}$C]verapamil the highest employed tariquidar dose (20 mg/kg) increased $K_{b,brain}$ to similar levels as in *Abcb1a/1b*$^{(-/-)}$ mice (Figure 3C), this was not the case for [$^{11}$C]-*N*-desmethyl-loperamide, for which $K_{b,brain}$ after 30 mg/kg tariquidar was significantly lower ($P < 0.01$) than $K_{b,brain}$ in *Abcb1a/1b*$^{(-/-)}$ mice (Figure 3D). We speculate that a possible explanation for this phenomenon may be competition for intracellular trapping in acidic lysosomes in brain parenchyma between the two weak bases tariquidar and [$^{11}$C]-*N*-desmethyl-loperamide.[36] With increasing doses tariquidar may increasingly compete with [$^{11}$C]-*N*-desmethyl-loperamide for lysosomal trapping, which may result in a decrease in brain uptake of [$^{11}$C]-*N*-desmethyl-loperamide and thereby prevent that the same extent of brain distribution is reached as in *Abcb1a/1b*$^{(-/-)}$ mice. Such a competition appears possible as we have shown in a previous study that tariquidar enters the brain when given at pharmacological doses (15 mg/kg) because it inhibits its own efflux transport by Abcb1a and Abcg2 at the BBB.[37] *In vivo* $IC_{50}$ of tariquidar for enhancement of brain distribution of (*R*)-[$^{11}$C]-verapamil in mice (1052 nM) was comparable with the $IC_{50}$ determined previously in rats (650 nM)[35] but lower than the $IC_{50}$ determined in humans (2248 nM).[19] This indicates that higher tariquidar plasma concentrations are needed in humans than in rodents to inhibit ABCB1 at the BBB. Plasma protein binding of tariquidar may differ between rodents and humans, but this is difficult to determine reliably since tariquidar is a highly plasma protein bound drug (unbound fraction in human plasma: 0.0063).[38] When correcting *in vivo* $IC_{50}$ values of tariquidar determined in mice for plasma protein binding of tariquidar, unbound tariquidar $IC_{50}$ values were comparable with the respective *in vitro* $IC_{50}$ values determined in Abcb1a-transfected cells ((*R*)-[$^{11}$C]verapamil, *in vivo* $IC_{50}$ 6.6 nM, *in vitro* $IC_{50}$ 17.9 nM; [$^{11}$C]-*N*-desmethyl-loperamide, *in vivo* $IC_{50}$ 8.4 nM, *in vitro* $IC_{50}$ 6.0 nM).

In order to assess the effect of ABCB1 expression levels at the BBB on brain distribution of ABCB1 substrates, we investigated heterozygous *Abcb1a/1b*$^{(+/-)}$ mice, which were shown to have about 50% lower Abcb1a expression levels at the BBB than wild-type mice.[39,40] Heterozygous *Abcb1a/1b*$^{(+/-)}$ mice showed much smaller increases in brain distribution of (*R*)-[$^{11}$C]verapamil and [$^{11}$C]-*N*-desmethyl-loperamide compared to wild-type mice than homozygous *Abcb1a/1b*$^{(-/-)}$ mice (Figures 3C and 3D). This observation has also been made by others for other substrates[40,41] and suggests that ABCB1 acts at high capacity to restrict brain entry of ABCB1 substrates and loss of 50% of ABCB1 function at the BBB is not sufficient to permit brain entry of ABCB1 substrates. This implies that >50% of ABCB1 at the BBB needs to be inhibited to obtain appreciable increases in brain distribution of (*R*)-[$^{11}$C]verapamil and [$^{11}$C]-*N*-desmethyl-loperamide. This further suggests that 2-fold differences in ABCB1 expression levels at the BBB as they have been found between mice and humans[24] will exert only a minor impact on the magnitude of ABCB1-mediated DDIs at the BBB. Consequently, (*R*)-[$^{11}$C]verapamil and [$^{11}$C]-*N*-desmethyl-loperamide are not very sensitive radiotracers to detect small (<50%) variations in ABCB1 expression/function at the BBB, when used without administration of an ABCB1 inhibitor.

PET measures total radioactivity in tissue and is not able to distinguish radiolabeled metabolites from radiolabeled parent compound. (*R*)-[$^{11}$C]Verapamil is metabolized in rodents mainly by *N*-demethylation giving [$^{11}$C]formaldehyde and related polar radiolabeled metabolites, which showed brain uptake in rats.[42] In humans, additionally *N*-dealkylation of (*R*)-[$^{11}$C]verapamil occurs, giving lipophilic radiolabeled metabolites ([$^{11}$C]D617, [$^{11}$C]D717), which were shown to be transported by ABCB1.[43] [$^{11}$C]-*N*-Desmethyl-loperamide shows little metabolism in humans,[44] but is extensively metabolized in mice giving the *N*-hydroxymethyl analogue as main radiolabeled metabolite, which is an ABCB1 substrate.[45] We analyzed radiolabeled metabolites of (*R*)-[$^{11}$C]verapamil and [$^{11}$C]-*N*-desmethyl-loperamide in plasma and brain of wild-type mice pretreated with either vehicle or tariquidar (15 mg/kg). For both radiotracers


DOI: 10.1021/acs.molpharmaceut.5b00168
*Mol. Pharmaceutics* 2015, 12, 3214−3225

radiolabeled metabolites were detected in plasma and brain (Table 2). However, the percentage of radiolabeled metabolites in brain was for both radiotracers lower in tariquidar treated than in vehicle treated animals, presumably because radiolabeled metabolites were not or were to a lesser extent transported by Abcb1a (Table 2). When considering total radioactivity, increases in $K_{p,brain}$ after tariquidar administration were similar for both radiotracers (Table 3). When correcting $K_{p,brain}$ values for radiolabeled metabolites in plasma and brain, increases were higher for [$^{11}$C]-*N*-desmethyl-loperamide than for (*R*)-[$^{11}$C]-verapamil. This was consistent with higher TRs observed *in vitro* in Abcb1a-transfected cells for [$^{3}$H]-*N*-desmethyl-loperamide than for [$^{3}$H]verapamil (see above). This demonstrates that radiotracer metabolism and brain uptake of radiolabeled metabolites may exert a pronounced impact on the magnitude of ABCB1-mediated DDIs (Table 3). Therefore, differences in metabolism of radiotracers between rodents and humans may have contributed to differences seen in ABCB1-mediated DDIs measured with PET.

It has been shown that under conditions of ABCB1 inhibition brain uptake of [$^{11}$C]-*N*-desmethyl-loperamide is dependent on CBF.[20,46] We therefore hypothesized that CBF may influence the magnitude of ABCB1-mediated DDIs by determining the extent of brain uptake of ABCB1 substrates after ABCB1 inhibition. This may account for species differences in ABCB1-mediated DDIs between rodents and humans[18] as rodents have higher CBF than humans.[47] Moreover, rodents usually undergo PET examinations under isoflurane anesthesia, which increases CBF.[48,49] In order to assess dependence of (*R*)-[$^{11}$C]verapamil and [$^{11}$C]-*N*-desmethyl-loperamide brain distribution on CBF, we tested isoflurane anesthetized and awake wild-type and *Abcb1a/1b*$^{(-/-)}$ mice (Table 4). We could show by using *N*-isopropyl-*p*-[$^{125}$I]iodoamphetamine, a high-extraction radiotracer whose brain uptake has been shown to correlate with CBF,[50] that CBF was approximately 1.6 times higher in isoflurane anesthetized than in awake animals (Table 4). While we detected for (*R*)-[$^{11}$C]verapamil no differences in $K_{b,brain}$ values between anesthetized and awake wild-type or *Abcb1a/1b*$^{(-/-)}$ mice, $K_{b,brain}$ values of [$^{11}$C]-*N*-desmethyl-loperamide were against our expectations significantly lower in anesthetized than in awake *Abcb1a/1b*$^{(-/-)}$ mice (Table 4). In order to test if these differences in radiotracer brain uptake between anesthetized and awake mice were due to differences in radiotracer metabolism, we compared metabolism of (*R*)-[$^{11}$C]verapamil and [$^{11}$C]-*N*-desmethyl-loperamide in groups of vehicle and tariquidar treated wild-type mice under short (5 min) and long (160 min) isoflurane anesthesia (Table 2). We observed no significant differences in (*R*)-[$^{11}$C]verapamil metabolism for the short and long anesthesia groups. However, for [$^{11}$C]-*N*-desmethyl-loperamide percentage of unchanged parent in plasma was significantly higher under short than under long anesthesia (Table 2). This suggested that isoflurane dose dependently alters [$^{11}$C]*N*-desmethyl-loperamide metabolism, which may have masked the effect of CBF on [$^{11}$C]*N*-desmethyl-loperamide brain distribution (assuming that brain distribution of radiolabeled metabolites is not or is to a lesser extent dependent on CBF). The effect of isoflurane on [$^{11}$C]*N*-desmethyl-loperamide metabolism may be caused by changes of hepatic blood flow or by alterations in the activity of metabolic enzymes.[51,52] When correcting total-radioactivity $K_{p,brain}$ values shown in Table 3 for radiolabeled metabolites of [$^{11}$C]*N*-desmethyl-loperamide we obtained significantly higher $K_{p,brain,dLOP}$ values in tariquidar treated mice under long than under short anesthesia, presumably due to higher CBF in the long anesthesia group. This suggests that under conditions of ABCB1 inhibition brain uptake of [$^{11}$C]*N*-desmethyl-loperamide but not (*R*)-[$^{11}$C]verapamil depends on CBF which may directly affect the magnitude of ABCB1-mediated DDIs. This does not exclude that other parameters of (*R*)-[$^{11}$C]verapamil brain distribution than $K_{b,brain}$ (i.e., the influx rate constant from plasma into brain $K_1$) may be dependent on CBF.[53] Moreover, isoflurane anesthesia may alter metabolism of radiotracers, which could also influence transporter-mediated DDIs.

We finally assessed protein binding of (*R*)-[$^{11}$C]verapamil and [$^{11}$C]-*N*-desmethyl-loperamide in mouse and human plasma (Table 5). We found small but significant differences in the percentages of non-protein bound (*R*)-[$^{11}$C]verapamil between mouse and human plasma, which may contribute to species differences in brain distribution of (*R*)-[$^{11}$C]verapamil. For [$^{11}$C]-*N*-desmethyl-loperamide no differences in plasma protein binding were found between mice and humans. Moreover, in agreement with previous results,[17,19−21,35] tariquidar did not change the percentage of non-protein bound (*R*)-[$^{11}$C]verapamil and [$^{11}$C]-*N*-desmethyl-loperamide in mouse plasma (Table 5).

In conclusion, we have identified a number of important factors, which are specific to PET experiments, including brain uptake of radiolabeled metabolites and anesthesia (see Table 1), which can exert a profound impact on the magnitude of ABCB1-mediated DDIs measured with PET. Therefore, we recommend that these factors be taken into consideration when interpreting species differences between rodents and humans in transporter-mediated DDIs.

## ■ ASSOCIATED CONTENT

### Supporting Information

The Supporting Information is available free of charge on the ACS Publications website at DOI: 10.1021/acs.molpharmaceut.5b00168.

Blood radioactivity concentrations for (*R*)-[$^{11}$C]verapamil and [$^{11}$C]-*N*-desmethyl-loperamide in vehicle and tariquidar treated wild-type mice; correlation between $K_{b,brain}$ and $V_T$ for (*R*)-[$^{11}$C]verapamil PET data in healthy human volunteers (PDF)

## ■ AUTHOR INFORMATION


### Corresponding Author

*Health & Environment Department, AIT Austrian Institute of Technology GmbH, 2444 Seibersdorf, Austria. Tel: +43 50550 3496. Fax: +43 50550 2136. E-mail: oliver.langer@ait.ac.at.


### Notes

The authors declare no competing financial interest.

## ■ ACKNOWLEDGMENTS


The authors wish to thank Maria Zsebedics for help in conducting the experiments. This work was supported by the Austrian Science Fund (FWF) [Grants P24894-B24, I1609-B24, F 3513-B20].


## ■ REFERENCES


(1) Kalvass, J. C.; Polli, J. W.; Bourdet, D. L.; Feng, B.; Huang, S. M.; Liu, X.; Smith, Q. R.; Zhang, L. K.; Zamek-Gliszczynski, M. J. Why clinical modulation of efflux transport at the human blood-brain barrier is unlikely: the ITC evidence-based position. *Clin. Pharmacol. Ther.* **2013**, *94*, 80−94.

(2) Schinkel, A. H.; Wagenaar, E.; van Deemter, L.; Mol, C. A.; Borst, P. Absence of the mdr1a P-Glycoprotein in mice affects tissue




DOI: 10.1021/acs.molpharmaceut.5b00168
*Mol. Pharmaceutics* 2015, 12, 3214−3225

distribution and pharmacokinetics of dexamethasone, digoxin, and cyclosporin A. *J. Clin. Invest.* **1995**, *96*, 1698−1705.
(3) Schinkel, A. H.; Wagenaar, E.; Mol, C. A.; van Deemter, L. P-glycoprotein in the blood-brain barrier of mice influences the brain penetration and pharmacological activity of many drugs. *J. Clin. Invest.* **1996**, *97*, 2517−2524.
(4) Schinkel, A. H.; Smit, J. J.; van Tellingen, O.; Beijnen, J. H.; Wagenaar, E.; van Deemter, L.; Mol, C. A.; van der Valk, M. A.; Robanus-Maandag, E. C.; te Riele, H. P.; et al. Disruption of the mouse mdr1a P-glycoprotein gene leads to a deficiency in the blood-brain barrier and to increased sensitivity to drugs. *Cell* **1994**, *77*, 491−502.
(5) Cutler, L.; Howes, C.; Deeks, N. J.; Buck, T. L.; Jeffrey, P. Development of a P-glycoprotein knockout model in rodents to define species differences in its functional effect at the blood-brain barrier. *J. Pharm. Sci.* **2006**, *95*, 1944−1953.
(6) Choo, E. F.; Leake, B.; Wandel, C.; Imamura, H.; Wood, A. J.; Wilkinson, G. R.; Kim, R. B. Pharmacological inhibition of P-glycoprotein transport enhances the distribution of HIV-1 protease inhibitors into brain and testes. *Drug Metab. Dispos.* **2000**, *28*, 655−660.
(7) Choo, E. F.; Kurnik, D.; Muszkat, M.; Ohkubo, T.; Shay, S. D.; Higginbotham, J. N.; Glaeser, H.; Kim, R. B.; Wood, A. J.; Wilkinson, G. R. Differential in vivo sensitivity to inhibition of P-glycoprotein located in lymphocytes, testes, and the blood-brain barrier. *J. Pharmacol. Exp. Ther.* **2006**, *317*, 1012−1018.
(8) Eyal, S.; Hsiao, P.; Unadkat, J. D. Drug interactions at the blood-brain barrier: fact or fantasy? *Pharmacol. Ther.* **2009**, *123*, 80−104.
(9) Sadeque, A. J.; Wandel, C.; He, H.; Shah, S.; Wood, A. J. Increased drug delivery to the brain by P-glycoprotein inhibition. *Clin. Pharmacol. Ther.* **2000**, *68*, 231−237.
(10) Kurnik, D.; Sofowora, G. G.; Donahue, J. P.; Nair, U. B.; Wilkinson, G. R.; Wood, A. J.; Muszkat, M. Tariquidar, a selective P-glycoprotein inhibitor, does not potentiate loperamide's opioid brain effects in humans despite full inhibition of lymphocyte P-glycoprotein. *Anesthesiology* **2008**, *109*, 1092−1099.
(11) Wulkersdorfer, B.; Wanek, T.; Bauer, M.; Zeitlinger, M.; Muller, M.; Langer, O. Using positron emission tomography to study transporter-mediated drug-drug interactions in tissues. *Clin. Pharmacol. Ther.* **2014**, *96*, 206−213.
(12) Hendrikse, N. H.; Schinkel, A. H.; de Vries, E. G.; Fluks, E.; Van der Graaf, W. T.; Willemsen, A. T.; Vaalburg, W.; Franssen, E. J. Complete in vivo reversal of P-glycoprotein pump function in the blood-brain barrier visualized with positron emission tomography. *Br. J. Pharmacol.* **1998**, *124*, 1413−1418.
(13) Sasongko, L.; Link, J. M.; Muzi, M.; Mankoff, D. A.; Yang, X.; Collier, A. C.; Shoner, S. C.; Unadkat, J. D. Imaging P-glycoprotein transport activity at the human blood-brain barrier with positron emission tomography. *Clin. Pharmacol. Ther.* **2005**, *77*, 503−514.
(14) Muzi, M.; Mankoff, D. A.; Link, J. M.; Shoner, S.; Collier, A. C.; Sasongko, L.; Unadkat, J. D. Imaging of cyclosporine inhibition of P-glycoprotein activity using $^{11}$C-verapamil in the brain: studies of healthy humans. *J. Nucl. Med.* **2009**, *50*, 1267−1275.
(15) Luurtsema, G.; Molthoff, C. F.; Windhorst, A. D.; Smit, J. W.; Keizer, H.; Boellaard, R.; Lammertsma, A. A.; Franssen, E. J. (*R*)- and (*S*)-[$^{11}$C]verapamil as PET-tracers for measuring P-glycoprotein function: in vitro and in vivo evaluation. *Nucl. Med. Biol.* **2003**, *30*, 747−751.
(16) Lubberink, M.; Luurtsema, G.; van Berckel, B. N.; Boellaard, R.; Toornvliet, R.; Windhorst, A. D.; Franssen, E. J.; Lammertsma, A. A. Evaluation of tracer kinetic models for quantification of P-glycoprotein function using (*R*)-[$^{11}$C]verapamil and PET. *J. Cereb. Blood Flow Metab.* **2007**, *27*, 424−433.
(17) Wagner, C. C.; Bauer, M.; Karch, R.; Feurstein, T.; Kopp, S.; Chiba, P.; Kletter, K.; Löscher, W.; Müller, M.; Zeitlinger, M.; Langer, O. A pilot study to assess the efficacy of tariquidar to inhibit P-glycoprotein at the human blood-brain barrier with (*R*)-$^{11}$C-verapamil and PET. *J. Nucl. Med.* **2009**, *50*, 1954−1961.
(18) Bauer, M.; Zeitlinger, M.; Karch, R.; Matzneller, P.; Stanek, J.; Jager, W.; Böhmdorfer, M.; Wadsak, W.; Mitterhauser, M.; Bankstahl, J. P.; Löscher, W.; Koepp, M.; Kuntner, C.; Müller, M.; Langer, O. Pgp-mediated interaction between (*R*)-[$^{11}$C]verapamil and tariquidar at the human blood-brain barrier: a comparison with rat data. *Clin. Pharmacol. Ther.* **2012**, *91*, 227−233.
(19) Bauer, M.; Karch, R.; Zeitlinger, M.; Philippe, C.; Römermann, K.; Stanek, J.; Maier-Salamon, A.; Wadsak, W.; Jäger, W.; Hacker, M.; Müller, M.; Langer, O. Approaching complete inhibition of P-glycoprotein at the human blood-brain barrier: an (*R*)-[$^{11}$C]verapamil PET study. *J. Cereb. Blood Flow Metab.* **2015**, *35*, 743−746.
(20) Kreisl, W. C.; Liow, J. S.; Kimura, N.; Seneca, N.; Zoghbi, S. S.; Morse, C. L.; Herscovitch, P.; Pike, V. W.; Innis, R. B. P-glycoprotein function at the blood-brain barrier in humans can be quantified with the substrate radiotracer $^{11}$C-N-desmethyl-loperamide. *J. Nucl. Med.* **2010**, *51*, 559−566.
(21) Kreisl, W. C.; Bhatia, R.; Morse, C. L.; Woock, A. E.; Zoghbi, S. S.; Shetty, H. U.; Pike, V. W.; Innis, R. B. Increased permeability-glycoprotein inhibition at the human blood-brain barrier can be safely achieved by performing PET during peak plasma concentrations of tariquidar. *J. Nucl. Med.* **2015**, *56*, 82−87.
(22) Fox, E.; Bates, S. E. Tariquidar (XR9576): a P-glycoprotein drug efflux pump inhibitor. *Expert Rev. Anticancer Ther.* **2007**, *7*, 447−459.
(23) Hsiao, P.; Sasongko, L.; Link, J. M.; Mankoff, D. A.; Muzi, M.; Collier, A. C.; Unadkat, J. D. Verapamil P-glycoprotein transport across the rat blood-brain barrier: cyclosporine, a concentration inhibition analysis, and comparison with human data. *J. Pharmacol. Exp. Ther.* **2006**, *317*, 704−710.
(24) Uchida, Y.; Ohtsuki, S.; Katsukura, Y.; Ikeda, C.; Suzuki, T.; Kamiie, J.; Terasaki, T. Quantitative targeted absolute proteomics of human blood-brain barrier transporters and receptors. *J. Neurochem.* **2011**, *117*, 333−345.
(25) Lazarova, N.; Zoghbi, S. S.; Hong, J.; Seneca, N.; Tuan, E.; Gladding, R. L.; Liow, J. S.; Taku, A.; Innis, R. B.; Pike, V. W. Synthesis and evaluation of [N-methyl-$^{11}$C]N-desmethyl-loperamide as a new and improved PET radiotracer for imaging P-gp function. *J. Med. Chem.* **2008**, *51*, 6034−6043.
(26) Baltes, S.; Gastens, A. M.; Fedrowitz, M.; Potschka, H.; Kaever, V.; Löscher, W. Differences in the transport of the antiepileptic drugs phenytoin, levetiracetam and carbamazepine by human and mouse P-glycoprotein. *Neuropharmacology* **2007**, *52*, 333−346.
(27) Luna-Tortós, C.; Fedrowitz, M.; Löscher, W. Several major antiepileptic drugs are substrates for human P-glycoprotein. *Neuropharmacology* **2008**, *55*, 1364−1375.
(28) Polli, J. W.; Wring, S. A.; Humphreys, J. E.; Huang, L.; Morgan, J. B.; Webster, L. O.; Serabjit-Singh, C. S. Rational use of in vitro P-glycoprotein assays in drug discovery. *J. Pharmacol. Exp. Ther.* **2001**, *299*, 620−628.
(29) Brunner, M.; Langer, O.; Sunder-Plassmann, R.; Dobrozemsky, G.; Müller, U.; Wadsak, W.; Krcal, A.; Karch, R.; Mannhalter, C.; Dudczak, R.; Kletter, K.; Steiner, I.; Baumgartner, C.; Müller, M. Influence of functional haplotypes in the drug transporter gene ABCB1 on central nervous system drug distribution in humans. *Clin. Pharmacol. Ther.* **2005**, *78*, 182−190.
(30) Pardridge, W. M.; Fierer, G. Blood-brain barrier transport of butanol and water relative to N-isopropyl-p-iodoamphetamine as the internal reference. *J. Cereb. Blood Flow Metab.* **1985**, *5*, 275−281.
(31) Loening, A. M.; Gambhir, S. S. AMIDE: a free software tool for multimodality medical image analysis. *Mol. Imaging* **2003**, *2*, 131−137.
(32) Kühnle, M.; Egger, M.; Müller, C.; Mahringer, A.; Bernhardt, G.; Fricker, G.; Konig, B.; Buschauer, A. Potent and selective inhibitors of breast cancer resistance protein (ABCG2) derived from the p-glycoprotein (ABCB1) modulator tariquidar. *J. Med. Chem.* **2009**, *52*, 1190−1197.
(33) Römermann, K.; Wanek, T.; Bankstahl, M.; Bankstahl, J. P.; Fedrowitz, M.; Müller, M.; Löscher, W.; Kuntner, C.; Langer, O. (*R*)-[$^{11}$C]verapamil is selectively transported by murine and human P-glycoprotein at the blood-brain barrier, and not by MRP1 and BCRP. *Nucl. Med. Biol.* **2013**, *40*, 873−878.
(34) Kannan, P.; Brimacombe, K. R.; Zoghbi, S. S.; Liow, J. S.; Morse, C.; Taku, A. K.; Pike, V. W.; Halldin, C.; Innis, R. B.; Gottesman, M. M.; Hall, M. D. N-desmethyl-loperamide is selective for P-glycoprotein


DOI: 10.1021/acs.molpharmaceut.5b00168
*Mol. Pharmaceutics* 2015, 12, 3214−3225

among three ATP-binding cassette transporters at the blood-brain barrier. *Drug Metab. Dispos.* **2010**, *38*, 917−922.
(35) Kuntner, C.; Bankstahl, J. P.; Bankstahl, M.; Stanek, J.; Wanek, T.; Stundner, G.; Karch, R.; Brauner, R.; Meier, M.; Ding, X. Q.; Müller, M.; Löscher, W.; Langer, O. Dose-response assessment of tariquidar and elacridar and regional quantification of P-glycoprotein inhibition at the rat blood-brain barrier using (*R*)-[$^{11}$C]verapamil PET. *Eur. J. Nucl. Med. Mol. Imaging* **2010**, *37*, 942−953.
(36) Kannan, P.; Brimacombe, K. R.; Kreisl, W. C.; Liow, J. S.; Zoghbi, S. S.; Telu, S.; Zhang, Y.; Pike, V. W.; Halldin, C.; Gottesman, M. M.; Innis, R. B.; Hall, M. D. Lysosomal trapping of a radiolabeled substrate of P-glycoprotein as a mechanism for signal amplification in PET. *Proc. Natl. Acad. Sci. U. S. A.* **2011**, *108*, 2593−2598.
(37) Bankstahl, J. P.; Bankstahl, M.; Römermann, K.; Wanek, T.; Stanek, J.; Windhorst, A. D.; Fedrowitz, M.; Erker, T.; Müller, M.; Löscher, W.; Langer, O.; Kuntner, C. Tariquidar and elacridar are dose-dependently transported by p-glycoprotein and bcrp at the blood-brain barrier: a small-animal positron emission tomography and in vitro study. *Drug Metab. Dispos.* **2013**, *41*, 754−762.
(38) Sugimoto, H.; Hirabayashi, H.; Amano, N.; Moriwaki, T. Retrospective analysis of P-glycoprotein-mediated drug-drug interactions at the blood-brain barrier in humans. *Drug Metab. Dispos.* **2013**, *41*, 683−688.
(39) Umbenhauer, D. R.; Lankas, G. R.; Pippert, T. R.; Wise, L. D.; Cartwright, M. E.; Hall, S. J.; Beare, C. M. Identification of a P-glycoprotein-deficient subpopulation in the CF-1 mouse strain using a restriction fragment length polymorphism. *Toxicol. Appl. Pharmacol.* **1997**, *146*, 88−94.
(40) Tang, S. C.; de Vries, N.; Sparidans, R. W.; Wagenaar, E.; Beijnen, J. H.; Schinkel, A. H. Impact of P-glycoprotein (ABCB1) and breast cancer resistance protein (ABCG2) gene dosage on plasma pharmacokinetics and brain accumulation of dasatinib, sorafenib, and sunitinib. *J. Pharmacol. Exp. Ther.* **2013**, *346*, 486−494.
(41) Dagenais, C.; Zong, J.; Ducharme, J.; Pollack, G. M. Effect of mdr1a P-glycoprotein gene disruption, gender, and substrate concentration on brain uptake of selected compounds. *Pharm. Res.* **2001**, *18*, 957−963.
(42) Luurtsema, G.; Molthoff, C. F.; Schuit, R. C.; Windhorst, A. D.; Lammertsma, A. A.; Franssen, E. J. Evaluation of (*R*)-[$^{11}$C]verapamil as PET tracer of P-glycoprotein function in the blood-brain barrier: kinetics and metabolism in the rat. *Nucl. Med. Biol.* **2005**, *32*, 87−93.
(43) Verbeek, J.; Syvänen, S.; Schuit, R. C.; Eriksson, J.; de Lange, E. C.; Windhorst, A. D.; Luurtsema, G.; Lammertsma, A. A. Synthesis and preclinical evaluation of [$^{11}$C]D617, a metabolite of (*R*)-[$^{11}$C]verapamil. *Nucl. Med. Biol.* **2012**, *39*, 530−539.
(44) Seneca, N.; Zoghbi, S. S.; Liow, J. S.; Kreisl, W.; Herscovitch, P.; Jenko, K.; Gladding, R. L.; Taku, A.; Pike, V. W.; Innis, R. B. Human brain imaging and radiation dosimetry of $^{11}$C-N-desmethyl-loperamide, a PET radiotracer to measure the function of P-glycoprotein. *J. Nucl. Med.* **2009**, *50*, 807−813.
(45) Seneca, N.; Zoghbi, S. S.; Shetty, H. U.; Tuan, E.; Kannan, P.; Taku, A.; Innis, R. B.; Pike, V. W. Effects of ketoconazole on the biodistribution and metabolism of [$^{11}$C]loperamide and [$^{11}$C]N-desmethyl-loperamide in wild-type and P-gp knockout mice. *Nucl. Med. Biol.* **2010**, *37*, 335−345.
(46) Liow, J. S.; Kreisl, W.; Zoghbi, S. S.; Lazarova, N.; Seneca, N.; Gladding, R. L.; Taku, A.; Herscovitch, P.; Pike, V. W.; Innis, R. B. P-glycoprotein function at the blood-brain barrier imaged using $^{11}$C-N-desmethyl-loperamide in monkeys. *J. Nucl. Med.* **2009**, *50*, 108−115.
(47) Yuen, N.; Anderson, S. E.; Glaser, N.; Tancredi, D. J.; O'Donnell, M. E. Cerebral blood flow and cerebral edema in rats with diabetic ketoacidosis. *Diabetes* **2008**, *57*, 2588−2594.
(48) Hendrich, K. S.; Kochanek, P. M.; Melick, J. A.; Schiding, J. K.; Statler, K. D.; Williams, D. S.; Marion, D. W.; Ho, C. Cerebral perfusion during anesthesia with fentanyl, isoflurane, or pentobarbital in normal rats studied by arterial spin-labeled MRI. *Magn. Reson. Med.* **2001**, *46*, 202−206.
(49) Gelman, S.; Fowler, K. C.; Smith, L. R. Regional blood flow during isoflurane and halothane anesthesia. *Anesth. Analg.* **1984**, *63*, 557−565.
(50) Temma, T.; Magata, Y.; Mukai, T.; Kitano, H.; Konishi, J.; Saji, H. Availability of N-isopropyl-p-[$^{125}$I]iodoamphetamine (IMP) as a practical cerebral blood flow (CBF) indicator in rats. *Nucl. Med. Biol.* **2004**, *31*, 811−814.
(51) Wood, M.; Woad, A. J. J. Contrasting effects of halothane, isoflurane, and enflurane on in vivo drug metabolism in the rat. *Anesth. Analg.* **1984**, *63*, 709−714.
(52) Reilly, C. S.; Merrell, J.; Wood, A. J.; Koshakji, R. P.; Wood, M. Comparison of the effects of isoflurane or fentanyl-nitrous oxide anaesthesia on propranolol disposition in dogs. *Br. J. Anaesth.* **1988**, *60*, 791−796.
(53) Deo, A. K.; Borson, S.; Link, J. M.; Domino, K.; Eary, J. F.; Ke, B.; Richards, T. L.; Mankoff, D. A.; Minoshima, S.; O'Sullivan, F.; Eyal, S.; Hsiao, P.; Maravilla, K.; Unadkat, J. D. Activity of P-glycoprotein, a beta-amyloid transporter at the blood-brain barrier, is compromised in patients with mild Alzheimer disease. *J. Nucl. Med.* **2014**, *55*, 1106−1111.


DOI: 10.1021/acs.molpharmaceut.5b00168
*Mol. Pharmaceutics* 2015, 12, 3214−3225